

Search for neutrino generated air shower candidates with energy $\geq 10^{19}$ eV and Zenith angle θ

Stanislav Knurenko^a, Igor Petrov^b, and Artem Sabourov^c

Yu. G. Shafer Institute of Cosmophysical Research and Aeronomy. 31 Lenin ave., Yakutsk, Russia

Abstract. The description of the methodology and results of searching for air showers generated by neutral particles such as high energy gamma quanta and astroneutrinos are presented. For this purpose, we conducted a comprehensive analysis of the data: the electron, the muon and the EAS Cherenkov light, and their response time in scintillation and Cherenkov detectors. Air showers with energy more than $5 \cdot 10^{18}$ eV and zenith angle $\theta \geq 55^\circ$ are selected and analyzed. Search results indicate a lack of air shower events formed by gamma-rays or high-energy neutrinos, but it does not mean that such air showers do not exist in nature; for example, experiments that recorded showers having a marked low muon content, i.e., “Muonless”, are likely to be candidates for showers produced by neutral primary particles.

1. Introduction

Air showers from neutrinos can be formed in any part of the atmosphere because of its physical properties, passing quite a long way through matter. As a rule—it’s strongly inclined showers formed near the detector, i.e., young showers. The basis of such showers is the electron-photon component that is scattered at large angles and, therefore, has high latency particles relatively to particles formed in the shower core. Therefore, in such events a large number of peaks of the electrons in the signal scanned from the scintillation detector should be expected [1–3].

The aim of our work was to search for extensive air shower (EAS) candidates produced by atmospheric neutrinos. In order to do this a large number of air showers with time sweep responses from scintillation detectors of different sizes and different energy thresholds have been analyzed [1,2].

Preliminary results of the data analysis of the Yakutsk array indicates the absence of EAS events produced by neutrinos, but it does not mean that such EAS do not exist. It requires a further collection of strongly inclined showers and careful analysis. This requires improving the methodology for recording and processing showers.

2. Search methodology of high energy gamma rays and astro-neutrinos

2.1. Longitudinal development of air showers: depth of maximum development X_{max}

Longitudinal shower development at the Yakutsk array were reconstructed through the registration of EAS Cherenkov light [4,5], using the mathematical apparatus used when solving inverse problems [6,7]. This allowed

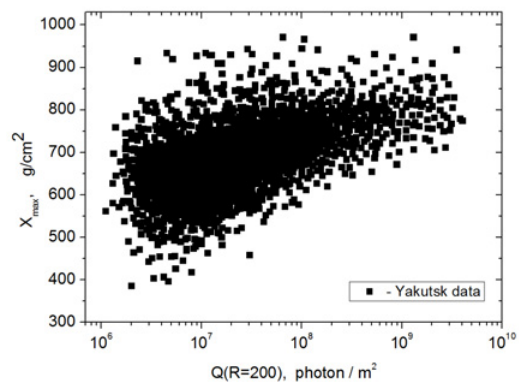


Figure 1. Dependence of X_{max} on the classification parameter $Q(200)$ —EAS Cherenkov light flux density at a distance of 200 m from the shower axis. Data obtained in 1973–2014.

us to find connection parameters describing the cascade curve X_{max} , N_{max} , the width of the cascade, q , with directly measured air shower characteristics at sea level, the shower energy E , the total number of charged particles and the shape of the lateral distribution of the Cherenkov light $R = I_g (Q_i / Q_j)$, where Q_i and Q_j are the flux densities of Cherenkov light at selected distances from the shower axis [8]. Using this method, an EAS database with reconstructed cascade curves was created. In addition, we selected air showers by X_{max} to study the depth of the maximum offset $dX_{max}/dI_g E$ and its fluctuation $\sigma_{X_{max}}$ for various energy intervals. Figure 1 shows the dependence of the distribution of X_{max} of individual showers from the classification parameter of the shower $Q(200)$ —the flux density of Cherenkov light at 200 m distance from the shower axis. Air shower energies can be determined by the formula (1) obtained by the energy balance method [9].

$$E_0 = (1.78 \pm 0.44) \cdot 10^{17} \cdot \left(\frac{Q(200)}{10^7} \right)^{1.01 \pm 0.04} \quad (1)$$

^a e-mail: knurenko@ikfia.ysn.ru

^b e-mail: igor.petrov@ikfia.sbras.ru

^c e-mail: tema@ikfia.ysn.ru

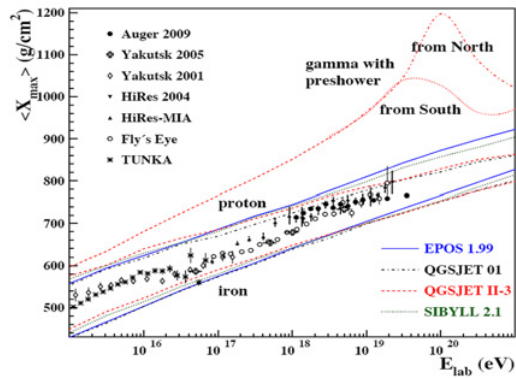


Figure 2. Dependence of X_{max} from energy. Experimental data comparison with calculations for different hadron interaction models (proton, iron nuclei and high-energy gamma ray).

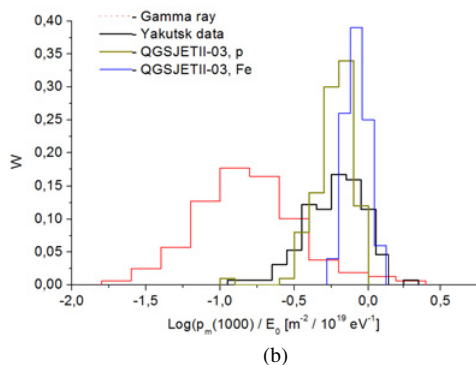
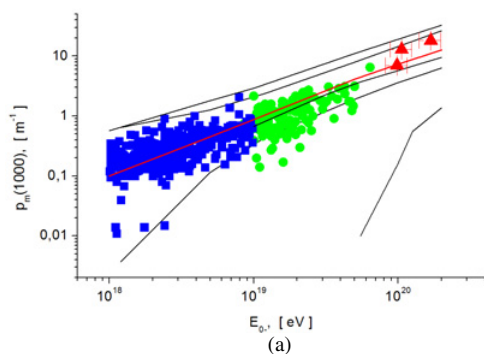


Figure 3. (a) Energy dependency of $\rho_{\mu}(1000)$ for observed events with energy 10^{18} – 10^{19} eV (squares) and 10^{19} – 10^{20} eV (triangles). Expected $\pm 1\sigma$ bounds of the distributions are indicated for proton, iron and gamma ray by different curves. (b) Fluctuations of $\rho_{\mu}(1000)/10^{19}$ value (eV) in showers with $E_0 > 10^{19}$ eV compared to simulation results (QGSjetII-03 + UrQMD) for protons, iron and photons.

Averaged Yakutsk data together with data from other arrays are shown in Fig. 2. In addition, there are calculations for some hadron interaction models for primary nuclei (proton and iron) and high-energy gamma rays. Figure 2 shows that the height of showers produced by gamma rays is lower by 150–180 g/cm² than proton produced showers with energy 10^{19} eV. In fact, the cascade curve X_{max} from gamma rays is near sea level at depth ~ 950 g/cm². In this case, there is a narrow cascade consisting mainly of electrons and photons with a very low muon content. This distinguishes showers produced by gamma rays from those produced by protons or nuclei of

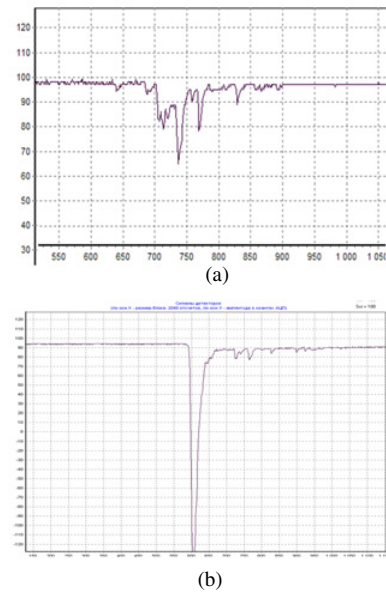


Figure 4. (a) Vertical air shower pulse. $E_0 = 1.7 \cdot 10^{19}$ eV, $\theta = 18^\circ$, $R = 1298$ m. Detector with area $s = 2$ m² and threshold $\varepsilon_{thr} \geq 10$ MeV. (b) Inclined air shower event. $E_0 = 2.4 \cdot 10^{19}$ eV, $\theta = 56^\circ$, $\psi = 200^\circ$, $R = 1000$ m.

any other element. We can assume that X_{max} can be used as the first criterion to search for EAS produced by gamma rays.

2.2. Number of muons in air showers

As mentioned in Sect. 2.1 gamma ray produced showers consist of a small number of muons. If the array detects muons then from the number of muons in the shower one can judge the nature of the primary particle i.e., its atomic weight (Fig. 3a and 3b).

In the Yakutsk array the proportion of muons in the shower is determined by the relation of the muon flux density at distances of 600 m and 1000 m to the total charged component $\rho_{\mu}/\rho_{\mu+e}$, since these parameters are measured with better accuracy than the total number of muons, N_{μ} , and charged particles, $N_{\mu+e}$, in showers with total energy $E_0 \geq 10^{18}$ eV. This will be the second criterion to search for showers produced by neutral particles that include gamma rays and neutrinos.

For these purposes, there are muon detectors at the Yakutsk array with areas of 1 m², 20 m² and 190 m², which record muons with a threshold energy $\varepsilon_{thr} \geq 1$ GeV for vertical showers and $\varepsilon_{thr} \geq 2$ GeV for inclined showers $\theta \geq 60^\circ$ [10]. The muon detectors are located on the array in such a way that in each shower they are measuring distances in the range from 100 to 1500 m, which allows us to estimate the fraction of muons at a particular distance from the shower axis. In particular, this analysis uses the estimated proportion of muons in showers with energies $\geq 10^{18}$ eV by the ratio of the normalized energy of the muon flux density to the density of charged particles measured by the surface scintillation detectors. Experimental results are shown in Fig. 3a, Fig. 3b [11–13]. Lines are calculations performed by the QGSJETII-03 model for protons, iron nuclei and primary gamma rays. The calculations take into account the instrumental errors and for this reason, in

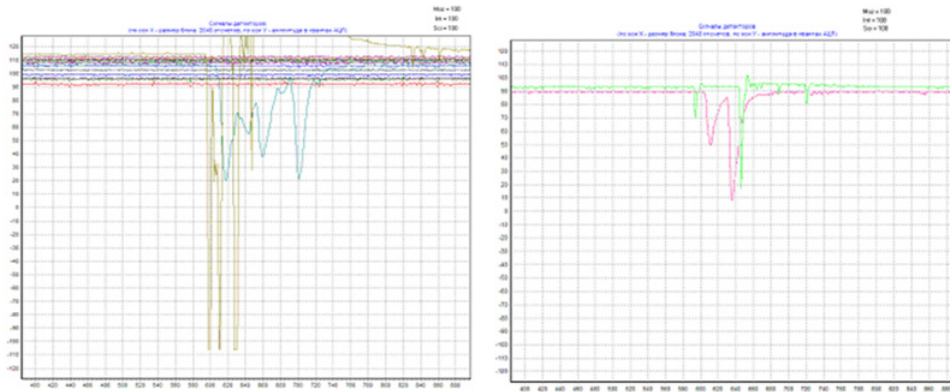


Figure 5. Distribution of pulses from electron and muon asymmetry in the air shower disc. Air shower event from 22.03.2009, $\theta = 32.4^\circ$, $\lg E_0 = 19.45$. a) $R = 549$ m b) $R = 886$ m.

Fig. 3a, double lines indicate the boundaries at 1σ expected areas measurements of muons in the case of different mass composition of primary particles.

Figure 3a shows that there is an overlapping region for gamma ray calculations (solid line) and the experimental data. In Fig. 3b there is also a similar overlap, which shows muon flux fluctuations at 1000 m from the shower axis, normalized to the shower energy (dots). This suggests the existence of high-energy gamma rays in the flow of cosmic particles, which produce EAS in the Earth's atmosphere.

2.3. Signal time sweep of surface and underground scintillation detectors

Air showers produced by different primary particles have a maximum development at different depths in the atmosphere. Because of this, some of the secondary particles (mostly electrons) lose energy to ionization in the air and are eliminated from the cascade process. So at sea level only certain types of particles will arrive: electrons, photons and muons in the case of inclined showers and only muons in the case of strongly inclined showers, which can be seen in the signal time sweep of the scintillation detectors. For primary gamma rays and neutrinos, the depth of the maximum is going to be near the level of observation and we can expect a scintillation detector response inherent in the electron-photon component of the shower. This is another criterion by which we can select showers produced by neutral particles.

Examples of scintillation detector responses in the case of vertical and inclined showers are given in Fig. 4a and Fig. 4b. These figures show that the shape of the pulse is different in each case. Vertical showers have many peaks, where each peak corresponds to a group or a single particle. As can be seen, all of the particles are distributed in time, i.e., they arrive with different delays with respect to the first particle. Most likely, it is due to the electrons scattered in the shower subcascades.

From Fig. 4b it is seen that for strongly inclined showers the pulse structure is different from vertical showers. It is a clear single, narrow pulse. The compactness of the arrival of these particles indicates that these particles are produced in the first interactions of the primary particle with air nuclei and in the course of decay processes of π^\pm -mesons, i.e., they are muons. The proof that single narrow pulses are muons passing through the scintillation detectors may be seen in Fig. 5, which shows

the pulses from particles passing through different amounts of material in the path to the detector, for example in over and under axial stations.

From Fig. 5, it follows that the number of peaks in the case of over axial stations are significantly reduced and is connected with the absorption of the electron-photon component of the shower because of the difference in particles path in the atmosphere. Thus strongly inclined air shower consist mainly of muons.

It must be noted that the signal shape asymmetry is significantly expressed in showers with zenith angles $\theta = 40^\circ$ – 55° . For large zenith angles, only a narrow single pulse is observed in the signal scan from air showers.

3. Experimental data analysis

In this work, we selected EAS events with $\theta \geq 60^\circ$ and energy above $5 \cdot 10^{18}$ eV for the pulse shape analysis. It was necessary for the shower axis to be within a circle with a radius of 1000 meters from the center of the Yakutsk array, where many of the monitoring stations and all underground stations for muon detection are located. In this case, the accuracy of the shower axis determination ($\sigma_x = 25$ m, $\sigma_y = 35$ m) was about the same and the best for all selected events. This also applies to the determination of the basic parameters of showers, such as the energy flux density of charged particles and muons at distances of 600 m and 1000 m, the zenith ($\sigma_\theta = 1.5^\circ$) and azimuth ($\sigma_\phi = 3.5^\circ$) angles. Selection of showers not only included the requirement of the pulse shape, but also its amplitude. Therefore, in the analysis we included showers with a pulse amplitude 5σ more than the average noise signal on the scan. The share of muons was determined by the ratio of the density of muons registered at distances of 600 m and 1000 m from the shower axis with respect to the flow of charged particles, registered at the same distances. The accuracy of determining each component is in the range of (15–25)% [14, 15].

Showers selected according to the criteria formed the basis of the data for analysis. A separate list was made up of showers with energies above $1 \cdot 10^{19}$ eV. The sample made was from data taken between 2000 and 2014 and included showers registered with both surface and underground detectors (charged particles and muons). An example of the lateral distribution of charged particles and muons of strongly inclined showers is shown in Fig. 6a.

Table 1. Strongly inclined showers with energy $E \geq 1 \cdot 10^{19}$ eV and $\theta \geq 60^\circ$.

Date	$\cos \theta$	θ	$\lg E$	Station number	number of peaks	$\rho_\mu / \rho_{\mu+e}$	QGSjetII-03
11.05.2000	0.266	74.6	19.63	33	1	0.91 ± 0.09	$0.84 \pm 0.03 / 0.89 \pm 0.03 / 0.20 \pm 0.03$
11.01.2002	0.322	71.2	19.08	27	1	0.92 ± 0.10	$0.84 \pm 0.03 / 0.89 \pm 0.03 / 0.20 \pm 0.03$
11.02.2002	0.330	70.7	19.04	27	1	0.94 ± 0.11	$0.84 \pm 0.03 / 0.89 \pm 0.03 / 0.20 \pm 0.03$
14.04.2002	0.319	71.4	19.10	32	1	1.11 ± 0.16	$0.84 \pm 0.03 / 0.89 \pm 0.03 / 0.20 \pm 0.03$
11.05.2006	0.437	64.1	19.05	42	1	1.06 ± 0.09	$0.84 \pm 0.03 / 0.89 \pm 0.03 / 0.20 \pm 0.03$
12.10.2006	0.445	63.6	19.17	49	1	1.17 ± 0.12	$0.84 \pm 0.03 / 0.89 \pm 0.03 / 0.20 \pm 0.03$
03.01.2007	0.495	60.3	19.43	35	1		$0.84 \pm 0.03 / 0.89 \pm 0.03 / 0.20 \pm 0.03$
15.05.2007	0.498	60.1	19.29	26	1		$0.84 \pm 0.03 / 0.89 \pm 0.03 / 0.20 \pm 0.03$
10.03.2008	0.425	64.8	19.18	49	1		$0.84 \pm 0.03 / 0.89 \pm 0.03 / 0.20 \pm 0.03$
21.02.2009	0.257	75.1	19.31	18	1	1.04 ± 0.07	$0.84 \pm 0.03 / 0.89 \pm 0.03 / 0.20 \pm 0.03$
21.03.2009	0.280	73.7	19.11	28	1		$0.84 \pm 0.03 / 0.89 \pm 0.03 / 0.20 \pm 0.03$
10.04.2009	0.401	66.4	19.17	41	1		$0.84 \pm 0.03 / 0.89 \pm 0.03 / 0.20 \pm 0.03$
25.05.2009	0.298	72.7	19.24	20	1		$0.84 \pm 0.03 / 0.89 \pm 0.03 / 0.20 \pm 0.03$
24.12.2009	0.402	66.3	19.21	44	1		$0.84 \pm 0.03 / 0.89 \pm 0.03 / 0.20 \pm 0.03$

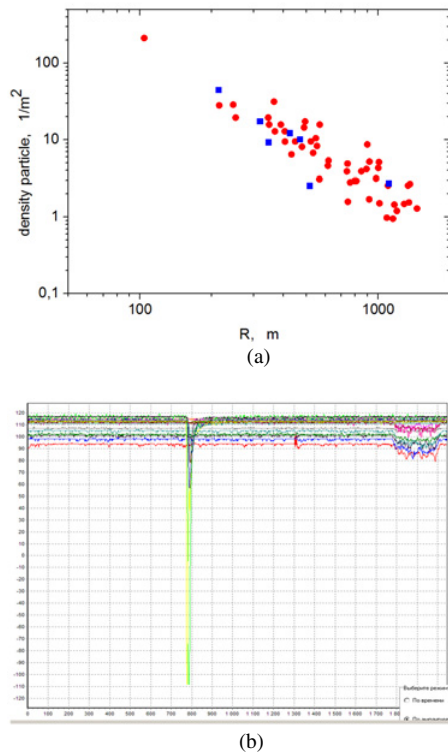


Figure 6. (a) Lateral distribution of the flux density of charged particles (red dots) and muons with $\varepsilon_{thr} \geq 2$ GeV (blue dots) in the shower with $E_0 = 1.5 \cdot 10^{19}$ eV and zenith angle $\theta = 64.8^\circ$. (b) Air shower signal scan, registered on 10.03.2008 by scintillation detectors (colored in darker colors) and Cherenkov light detectors (brighter colors).

It is not difficult (Fig. 7) to notice that the readings from the surface and underground detectors are equal, i.e., the same component of air showers is registered high-energy muons. On the signal scan, there are pulses from multiple scintillation detectors (colored in dark color) and by Cherenkov light detectors (brighter colors) (Fig. 7b). The shower front arrives at the detectors at the same time—this can be seen on the pulse rise time. The amplitudes of the Cherenkov light detector is greater than the amplitude registered by the scintillation detectors. Practically there are not many particles in the shower disk after passing

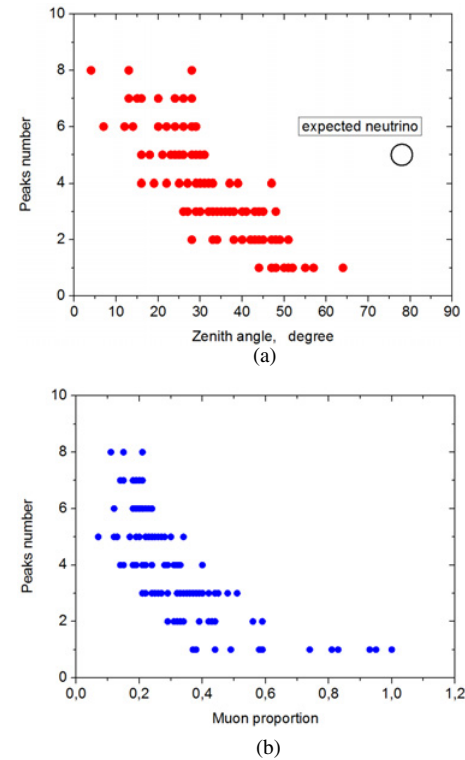


Figure 7. Number of peaks in the time sweep of scintillation detectors. a) Surface scintillation detector with threshold 10 MeV plotted against zenith angle b) underground scintillation detector with $\varepsilon_{thr} \geq 1$ GeV.

through the thickness of two atmospheres, and these particles are most likely high-energy muons. They arrive at sea level in a compact group, which forms a single and sufficiently narrow pulse. As can be seen, there is a strong variation in the detector readings for strongly inclined showers. This is due to the influence of the magnetic field on charged particles and the accuracy of locating the shower axis because of the significant asymmetry of the lateral distribution of the muons (Fig. 5a, Fig. 5b).

Characteristics of the largest showers are given in Table 1. These and other showers were included in this analysis to search for EAS candidates produced by neutral particles.

In Table 1, $\rho_{\mu}/\rho_{\mu+e}$ is for the distance 600 m from shower axis. In the case of QGSjetII-03, calculations are for $p/Fe/\gamma$ for energy $E = 10^{19}$ eV and $\theta \geq 60^\circ$.

Figure 7 shows the dependence of the number of peaks in the time sweep response of the scintillation detector from the zenith angle of the shower arrival (Fig. 7a) and from the proportion of muons at a distance of 600 meters from the EAS axis (Fig. 7b).

It can be seen that the number of peaks in the signal scan (Fig. 7a) strongly depends on the zenith angle. In the case of vertical showers with $\theta \leq 30^\circ$ and moderate distances from the shower axis, the number of peaks ranges from eight to four, and starting from zenith angles $\theta \geq 59^\circ$ there is only a single peak in the signal scan. The proportion of muons increases significantly with zenith angle and reaches almost 100% for $\theta \geq 60^\circ$. The observed pattern can be used as a sort of search criteria for air shower produced by neutral particles. For example if an EAS has a depth of maximum near sea level, $X_{\max} = (800-1000)$ g/cm², the number of muons is small and there are a large number of peaks in the signal scan at zenith angle $\theta \geq 60^\circ$ we can assume that this shower was produced by a neutral particle—gamma ray or neutrino - with a high probability. In Fig. 7a, this region is marked by a large circle. Thus, this work suggests that the search criteria for primary particles with characteristics different from protons and other nuclei may be suitable for such an analysis.

4. Conclusion

1944 EAS events with energy above $5 \cdot 10^{18}$ eV and $\theta \geq 60^\circ$ were registered over 15 years of continuous observations at the Yakutsk array. With the methodology suggested above, a comprehensive analysis of charged particles, muons and Cherenkov light data was carried out including time sweep in underground and surface scintillation detectors. The dependence of the shape of the scintillation detectors response in the time sweep on the zenith angle was studied. A characteristic feature was that there were many peaks in vertical showers and only a single peak in strongly inclined showers [2]. Use of the Cherenkov component of the shower in the analysis and reconstruction of the longitudinal shower development [5, 8] indicated a direct relationship of the peaks in the time sweep of the scintillation detector with the longitudinal development of the shower and number of muons in the shower. All this is well illustrated by the data shown in Figs. 7a and 7b.

A multi component analysis of air showers using the above described criteria, found no showers produced by gamma rays or neutrinos. At the same time, QGSJETII-03 model calculations for primary protons, iron nuclei and gamma rays (Figs. 2, 3a and 3b) tells us that if fluctuations of the muon measurements within 1σ are taken into account, the probability of detecting air showers produced by neutral particles exist. “Muonless” showers detected at the Yakutsk array can be considered as candidates for such showers [16].

References

- [1] S. Knurenko, Z. Petrov and Yu. Yegorov, J. Phys.: Conf. Ser. **409**, 012090 (2013) doi: 10.1088/1742-6596/409/1/012090
- [2] S. Knurenko and A. Saburov, Proc. of the 33th International Cosmic Ray Conference, Rio-de-Janeiro, 0055 (2013)
- [3] G.I. Rubtsov et al. EPJ Web of Conferences **53**, 05001 (2013) doi: 10.1051/epjconf/20135305001
- [4] M.N. Dyakonov, S.P. Knurenko, V.A. Kolosov et al. Nuclear Instruments and Meth-s in Phys. Rec. Amst. **A248**(4), p. 224–226 (1986)
- [5] S.P. Knurenko, V.A. Kolosov, Z.E. Petrov. Proc. 27-th ICRC, Hamburg (Germany) **1**, p. 157–160 (2001)
- [6] A.N. Tihonov, V.Ya. Arsenin. *Methods for solving ill-posed problems* (Science, Moscow, 1979), p. 286
- [7] V.A. Kochnev. Proc. of conference “The use of computers in control problems”, 62–71 (1985)
- [8] S.P. Knurenko. Ph. D. work, Yakutsk (2003)
- [9] S.P. Knurenko, A.A. Ivanov, I.Ye. Sleptsov, A.V. Sabourov. JETP Lett. **83**, 563–567 (2006)
- [10] V.P. Artamonov, B.N. Afanasyev, A.V. Glushkov. Bulletin of RAS. Physics Ser. **58**, 92–97 (1994)
- [11] S.P. Knurenko et al. Nuclear Physics B (Proc. Suppl.) **151**, 92–95 (2006)
- [12] S.P. Knurenko, A.A. Ivanov, M.I. Pravdin, A.V. Sabourov and I.Ye. Sleptsov. Nucl. Phys. B (Pros. Suppl.) **175-176**, 201–206 (2008)
- [13] S.P. Knurenko, A.V. Sabourov. Nuclear Physics B (Proc. Suppl.) **196**, 319–322 (2009)
- [14] M.N. Dyakonov, A.A. Ivanov, S.P. Knurenko et al. Proc. 17th ICRC **6**, 78–81 (1981)
- [15] Stanislav Knurenko et al. EPJ Web of Conferences **99**, 04001 (2015)
- [16] V.A. Kolosov et al. Proc. 31th ICRC, 287 (2009)